https://doi.org/10.5194/tc-2022-241
Preprint. Discussion started: 13 February 2023


The Cryosphere Discussions
Open Access
EGU

# Variations of ice thickness in a reservoir along Irtysh River: field measurement and regression analysis

Chuntan Han[1], Chao Kang[2], Chengxian Zhao[3], Jianhua Luo[3], Rensheng Chen[1]

[1]Northwest Institute of Eco-Environment and Resources, Chinese Academy of Sciences, Lanzhou, 730000, China.
[2]ParklandGEO Ltd., Sherwood Park, T8H 2W8, Canada.
[3]Irtysh River of Xinjiang Investment and Development (Group) Co. LTD, Ürümqi, 650105, China.

*Correspondence to*: Chao Kang (ckang3@ualberta.ca)

**Abstract:** This paper presents the analysis results of temperatures collected at three monitoring stations which were used to study ice freezing and thawing processes on a reservoir along Irtysh River. The measured temperatures were comprehensively analyzed and correlated with air temperature measured at a meteorological station. The results showed that air temperature was closely related to temperature at the ice surface, e.g., $T_{40}$, $T_{20}$ and $T_0$, and temperatures in ice almost increased linearly with depth. In addition, ice thicknesses were calculated based on measured temperatures along arrays of temperature and compared with that calculated using a simplified Stefan's model. The results indicated that ice thickness varied spatially and temporally, and Stefan's model overestimated the ice thicknesses with a maximum discrepancy of 12 cm. Moreover, the calculated ice thickness was correlated with temperatures, variations of temperature and accumulated freezing degree days (AFDD) based on Pearson correlation analysis, showing that ice thickness was proportional to AFDD with a coefficient of 0.89, and negatively correlated with $T_0$, $T_{-3}$, and $T_{ice(c)}$ with coefficients of -0.69, -0.73 and -0.62, respectively. Therefore, linear and non-linear models were proposed, which were validated using datasets from three stations in Russia and Finland, demonstrating that the linear model incorporating AFDD and $T_0$ can capture local ice freezing and thawing processes with a relatively minor discrepancy, and the results were consistent at different stations. The paper provides an approach to comprehensively study the ice formation process and a practical model to calculate local ice thickness.

**Keywords**: ice thickness, temperature, Pearson correlation analysis, regression analysis, linear model.

https://doi.org/10.5194/tc-2022-241
Preprint. Discussion started: 13 February 2023


The Cryosphere Discussions
Open Access
EGU

## 1 INTRODUCTION

More than half of rivers and reservoirs in the northern hemisphere can form ice above moving water (Akyurt et al. 2002; Deng et al. 2020). The freezing period can be even more than half year. As an important aspect of winder hydrology, the freezing of water seasonally behind a dam can affect the operation of the water conservancy projects and apply additional pressure on water conservancy projects (Bouaanani et al. 2004; Hellgren et al. 2020; Hicks 2016). Factors affecting ice thickness include air temperature, flow velocity/fluctuating rate of water level, chemical components in the water, water depth, water area, etc. Therefore, researchers investigated the ice formation process and predict the potential ice thickness using different approaches. The most common methods are field monitoring and numerical modelling.

The ice thickness is commonly monitored by drilling holes and installing arrays of temperature along vertical profiles in ice (Aslamov et al. 2021; Cao et al. 2017; Murfitt et al. 2018; Ding and Mao 2021; Cao 2021). In terms of drilling holes, a ruler was in general penetrated the drilled hole to measure the ice thickness manually. The maximum depth can reach up to 4 to 10 m below the ice surface. The limitations are dataset was very small and very pricy in data collection. In addition, access to the ice surface can refrain from drilling holes. For the direct monitoring approach, temperature sensors were installed before ice was formed. The temperature dataset was collected in the datalogger, which was then transferred to a database for analysis (Aslamov et al. 2021; Cao et al. 2017; Howell et al. 2016). In this process, loading cells and sensors for solar radiation and wind speed can also be attached to a hydraulic structure or monitoring sensor, respectively, to assess the potential impact of the freezing process on reservoir dams (Hellgren et al. 2020). The advantage of the direct approach was that installing monitoring station can be completed before the freezing process. However, this method is applicable for small-scale monitoring, and monitoring resolution was limited by the spacing between sensors. In addition, it is challenging to stabilize the monitoring station before the freezing process.

For the indirect monitoring approach, remote sensing technology was generally adopted based on high-resolution air photos without physically measuring the ice thickness. This approach is very helpful for large-scale monitoring. However, for small-scale monitoring, air drones can be used to obtain ice thickness at a specified date. However, the accuracy of results heavily relies on the resolution of air photos and the results should be verified by drilling holes in ice. Therefore, it was commonly used for ice monitoring in ocean area. Another technology that was used in monitoring ice thickness was based on sonar technology, which is based on acoustic reflection. The most commonly used tool was SWIP system from ASL Environmental Sciences. The advantages are that ice thickness and water depth can be monitored. However, the reference point must be installed on river/lake beds (Aslamov et al. 2021; Braga et al. 2012; Deng et al. 2020; Xie et al. 2022).

Typically, there are three approaches to studying the ice formation process: a full energy budget, a linear heat transfer approximation and a simple temperature index (Hicks 2016; Otto et al. 2022). Zhaka et al. (2021) comprehensively reviewed the models used in calculating ice thickness. In practice, the degree day model proposed by Stefan was commonly used (Alexiades and Solomon 2018; Murfitt et al. 2018; Werder et al. 2020). In the Stefan's model, accumulated freezing degree days (AFDD) calculated from the local meteorological station were used and two

https://doi.org/10.5194/tc-2022-241
Preprint. Discussion started: 13 February 2023


empirical coefficients were included in the model and ranges were suggested based on field monitoring data. Bilello (1960) divided calculation into two steps: the freezing process and the decaying process. In the decaying process, accumulated thawing degree days (ATDD), instead of AFDD, was adopted. The discrepancy between the calculated ice thickness and that measured was less than 5 cm for estimating ice thickness in central Ontario, Canada (Murfitt et al. 2018). However, determining the empirical coefficient is very challenging and experience-based (Otto et al. 2022; Zhaka et al. 2021). Hao et al. (2017) calibrated the Stefan's model for ice thickness calculation in Yellow River, China with a power law equation, which incorporated AFDD, river surface velocity and three empirical coefficients. Unfortunately, the proposed model was not verified by other datasets.

The Stefan's model has been widely used in estimating ice thickness worldwide with two empirical coefficients. In Stefan's model, it was considered that ice surface temperature ($T_0$) and air temperature ($T_{air}$) were identical. However, few of them has investigated the correlation between $T_0$ and $T_{air}$. In addition, variation in ice thickness was always neglected on a small scale. Therefore, this research aims to monitor the temperatures close to ice surface at three stations on a reservoir along Irtysh River, which is comprehensively analyzed, and ice thicknesses, including average ice thickness and daily ice thickness, are calculated based on the measured temperatures. Pearson correlation coefficients between temperatures and ice thickness are calculated to explore the factors affecting ice thickness. Based on the selected factors from Pearson correlation analysis, three linear models and a non-linear model are proposed and compared based on mean absolute error (MAE), mean squared error (MSE) and root-mean-square error (RMSE). The model with the best performance in estimating ice thickness is also verified using the dataset from three stations in Russia and Finland. This research provides a practical model to calculate local ice thickness with air temperature and temperature at ice surface incorporated

## 2 STUDY AREA AND METHODOLOGY

The study area is located in Irtysh River of Xinjiang Province, China and temperatures were measured using three arrays of temperature at three stations: M1, M2 and M3 (Figure 1). Ice thickness was calculated by analyzing the temperature at each time step which was 30 minutes. Pearson correlation analysis together with evaluation indices were also introduced in the following sections.

### 2.1 Study area

Irtysh River Basin is a tributary that flows into the Arctic Ocean, which is one of three primary river basins in Xinjiang Province, China, with an area of $5.27\times10^4$ km$^2$. The study area is located on one of the reservoirs along Irtysh River (Figure 1), and the functions were to accommodate irrigation, power generation as well as drinking water to local people. Ice in the study area started to form in December and decay in March. The ice covers the reservoir sometimes up to five months in a year. Therefore, investigating the freezing and thawing characteristics of ice during this period, including daily ice thickness, variation of ice thickness every day, etc., are critical to the safe operation of the reservoir. Three arrays of temperature were installed at M1 and M2 on December 18, 2021, and at M3 on January 20, 2022 (Figure 1). M1 was installed 3 m north side of the deck, while M2 was 3 m west of the deck. M3 was installed after ice was formed and 30 m west of the deck (Figure 1). For each monitoring profile, the monitoring chain was composed

https://doi.org/10.5194/tc-2022-241
Preprint. Discussion started: 13 February 2023




of 47 sensors: two of them were above the water surface while the rest of them were placed below the water surface with a spacing of 3 cm for 40 of them and 10 cm for the deepest five sensors (Figure 1). Figure 2a shows the monitoring instrument in field and schematic diagram of the close view of the array of temperature (Figures 2b and 2c).

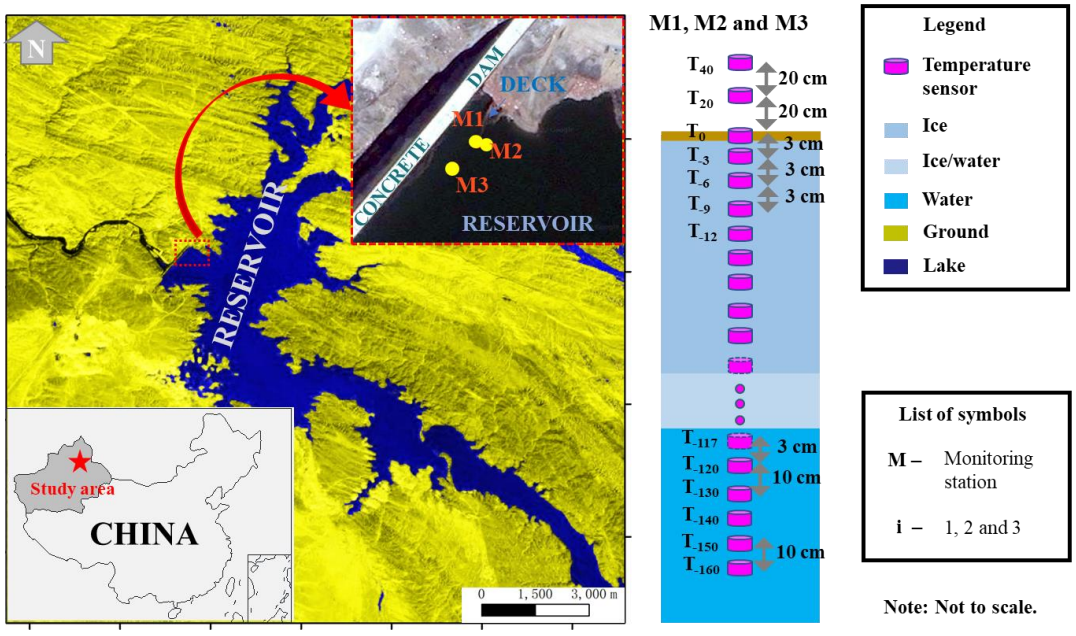


**Figure 1: Location of monitoring stations and configuration of sensors (© Google Maps 2022)**

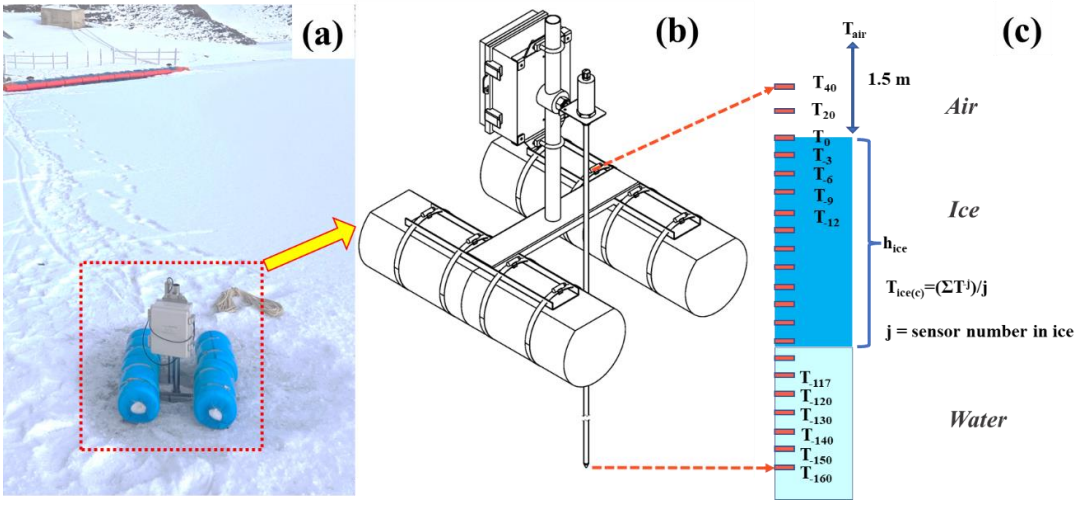


**Figure 2: Monitoring instrument in the field and schematic diagram showing the symbols in the analysis**

https://doi.org/10.5194/tc-2022-241
Preprint. Discussion started: 13 February 2023


### 2.2 Temperature measurement

In this study, $T_{air}$ along with $T_{40}$ and $T_{20}$ were collected at a frequency of 30 minutes starting from December 18, 2021, to March 29, 2022 using temperature-sensing resistance thermometer at M1 and M2. Air temperature, $T_{air}$, was collected from a meteorological station located approximately 30 km northeast of the reservoir at a frequency of 5 minutes. The monitoring information includes temperatures at M1, M2 and M3, the temperature of the control panel of data collection setup, locations of monitoring setup, and air moisture.

Temperature-sensing resistance thermometer on the monitoring array was developed by the State Key Laboratory of Froze Soil Engineering, Chinese Academy of Sciences (CAS), China (Figure 2) and was calibrated at the State key laboratory of frozen soil engineering (SKLFSE), China. The principle of the thermometer was to measure the variation of electrical resistance of water and the resolution was ±0.05 °C. Electrical resistivity was initially measured using a Fluke meter (accuracy of 0.05%, model: 289, Fluke Corporation, Everett, WA) and then was converted into temperature values. A datalogger (model: CR6, Campbell Scientific Inc., Logan, UT) was installed to automatically record the temperatures. The temperature chain was connected to the datalogger using SDI-12 output. The monitoring setup was powered by a solar panel, and the collected information was automatically transferred to a remote database. Besides, the thickness of the ice was manually measured in the close vicinity of M3 using a ruler on January 18, 2022. The monitoring station M3 was located on a floating platform, approximately 30 m away from the deck. An array of digital thermometer (DS18B20) was installed, which has an operating temperature range of -55°C to +125°C and was with an accuracy of ±0.5°C over the range of -10°C to +85°C. An adjustable pontoon was placed at the top of the temperature chain, equipped with a DTU and GPS module, to transmit data to local server and monitor the movement of ice in the reservoir. The entire system is powered by 3V dry cell battery, with extremely low power consumption and simple structure, which can accommodate continuous monitoring in the field for a long time.

### 2.3 Ice thickness calculation

For calculating ice thickness based on measured data, the ice water surface was identified at the change of temperature from that below zero degrees to a value that is above zero degrees. The field ice thickness was calculated based on the measured water/ice temperatures along the three sensor arrays. As the spacing between sensors right below the water/ice surface was 3 cm, the calculated ice thickness was with a maximum 3 cm discrepancy with the true ice thickness, which can be improved by decreasing the spacing. Daily ice thickness was averaged based on the calculated ice thickness at different time stages in a day.

Ice thickness was simulated using Stefan (1890)'s model. AFDD was calcualted based on avarge, maximum and minimum temperatures for comparision purpose. Stefan (1890) proposed an equation to estimate the ice thickness based on the assumption that $T_{air}$ is equal to $T_0$ and temperature at the bottom of the ice is equal to zero degrees. An equation is proposed based on thermal balance under ice, which is

$$\lambda \, d\theta/dh \, dt = L\rho dh(0 < h(t) < \quad (1)$$

The boundary condition is

https://doi.org/10.5194/tc-2022-241
Preprint. Discussion started: 13 February 2023


$$h(0) = 0 \tag{2}$$

Rearranging equation [1] yields

$$\frac{dh}{dt} = \frac{\lambda d\theta}{L\rho h} \tag{3}$$

Integrating equation [3] generates

$$h^2 = \frac{2\lambda}{L\rho}\int_0^t (\theta_t - \theta_a\,(t))dt \tag{4}$$

where $t$ is time; $h$ is ice thickness (cm); $\theta_a$ is air temperature (°C); $\theta_t$ is freezing temperature (°C); $\lambda$ is thermal conductivity of the solid ice (W m$^{-1}$ °C$^{-1}$); $\rho$ is ice density (kg/m$^3$); and $L$ is latent heat of formation (kJ kg$^{-1}$). Defining

$$\alpha = \frac{2\lambda}{L\rho} \tag{5}$$

$$AFDD = \sqrt{\int_0^t (\theta_t - \theta_a\,(t))dt} \tag{6}$$

Equation [4] becomes

$$h = \alpha\sqrt{AFDD} \tag{7}$$

where $\alpha$ is named as the growth rate coefficient (m °C$^{-0.5}$ d$^{-0.5}$), and *AFDD* is accumulated freezing degree days (°C d).

A model was proposed by Lebede (1938), which was simplified from Stefan's ice thickness model for sea ice. The model consists of two processes: freezing and decay. In the freezing process, the ice thickness was calculated using

$$h_F = \beta_F AFDD^{\gamma} \tag{8}$$

where $\beta_F$ and $\gamma$ are constants that can be empirically determined (Comfort and Abdelnour 2013). $\beta_F$ ranges from 0.014 to 0.17 for an average river with snow and from 0.017 to 0.024 for an average lake with snow (Hicks 2016).

To estimate ice thickness during the process of ice decay, linear regression method was used. Bilello (1960) developed an equation that uses ATDD to estimate the rate of sea ice decay (2):

$$h_D = I_m - \beta_F ATDD \tag{9}$$

where, $I_m$ is maximum ice thickness (mm), ATDD is the accumulated thawing degree days (°C d), and $\beta_T$ is the rate of ice decay (cm/ ATDD).

### 2.4 Pearson coefficient of correlation and indices used to evaluate the model performance

Pearson coefficient of correlation was generally used to demonstrate the linear correlation between two datasets. The coefficient was defined as the ratio between the covariance of two variables and the product of their standard deviations. The result always has a value between −1 and 1. If the correlation coefficient is between 0 and 1, it means

https://doi.org/10.5194/tc-2022-241
Preprint. Discussion started: 13 February 2023


the two variables are positively correlated, while the correlation coefficient between 0 and -1 indicates a negative correlation.

Linear regression of dataset was studied using a program developed using programming language, Python. To evaluate the performance of the training results, the Mean Average Error (MAE), the Mean Squared Error (MSE) or the Root Mean Squared Error (RMSE) are used as criteria.

## 3 RESULTS

Since ice thickness is calculated based on the measured temperatures, the variation of $T_{air}$ along with temperatures close to ice surface and in the ice and water, i.e., $T_{40}$, $T_{20}$ and $T_0$, are comprehensively analyzed. The correlations between $T_{air}$ and temperatures close to ice surface are investigated. Ice thickness, $h_{ice}$, is calculated based on an assumption that temperatures at the interface between water and ice is zero degrees. The ice thickness is also simulated using Stefan's model. Variation of ice thickness in a day and temperatures along the depth of ice are explored.

### 3.1 Temperatures

#### 3.1.1 Ice temperature and air temperature (profiles at different times)

Figure 3 shows the variation in daily temperature at monitoring stations, i.e., M1, M2 and M3. The lowest $T_{air}$ along with the lowest temperatures in all monitoring stations were observed at the end of January 2022. The lowest $T_{air}$ was approximately -17°C while the lowest $T_{40}$ were -12°C, 0°C, -16°C and $T_0$ were -6.5°C, -12°C and -6.5°C at M1, M2 and M3, respectively.

The temperatures at M2 were always higher than that measured at M1. The temperature measured at M3 was consistently smaller than that at stations M1 and M2 which were close to the reservoirs shore. The differences between M1 and M2, and M2 and M3 were smaller in the ice than that above ice surface. The reason was that heat conduct in the ice was less likely affected by the movement of airflow above the ice surface. In addition, the variation of temperature above the ice surface was more considerable than the variation in the ice.

The measured air temperature overall was lower than averaged $T_{40}$, $T_{20}$, $T_0$ and $T_{-3}$. There are two reasons contributing to the difference between $T_{air}$, measured 1.5 m above the ground surface, and temperatures close to water/ice surface. The first reason was the presence of the snow can reduce heat loss below and at water/ice surface. Air temperature was measured 1.5 m above the ground surface. The airflow around the temperature sensor in the instrument shelter moved faster than that close to the ground surface, which can accelerate the loss of thermal energy. The last reason was solar energy may transfer to temperature sensors close to the ground surface and in the water/ice. The instrument shelter limited the direct solar radiation. Therefore, the air temperature was generally lower than that in all monitoring stations.

Generally, air temperature was adopted to directly estimate the ice thickness (Murfitt et al. 2018; Hellgren et al. 2020). However, a significant difference exists between $T_{air}$ and the temperature close to the ice surface. The daily average $T_{air}$ was compared with the daily average temperature at each depth on the monitoring arrays. For monitoring stations M1 and M2, the maximum difference in temperature varied from -11°C to -14°C and from -15°C to -20°C, respectively,

https://doi.org/10.5194/tc-2022-241
Preprint. Discussion started: 13 February 2023




while the maximum difference in temperature between $T_{air}$ and temperatures at M3 was comparatively small, ranging from -6°C to -12°C. A relatively more considerable difference in temperature was noticed at M2 than at M1 resulted from the impact of the deck, which can reflect sunlight. M1 was installed on the north side of the deck. Therefore, limited daylight can affect the temperature of the array at M1, resulting in a relatively smaller difference in temperature between temperature at M1, $T^1$ and $T_{air}$. The temperature at the monitoring station M3, $T^3$, was always closer to $T_{air}$ compared to the temperature at M1 and M2, as no shelter or barrier affected the solar energy. The difference between $T^1$ and $T_{air}$ was mostly from the gradient distribution of temperature.

The difference between the temperatures below the ice surface was smaller than that above the ground surface at M1 and M2. In addition, the variation of the difference between $T_0^1$ and $T_{air}$ decreases when air temperature increases from December to March, resulting from snow melting at the ice surface, which can be further verified by the decrease of $T_{air}$ - $T_0^1$.

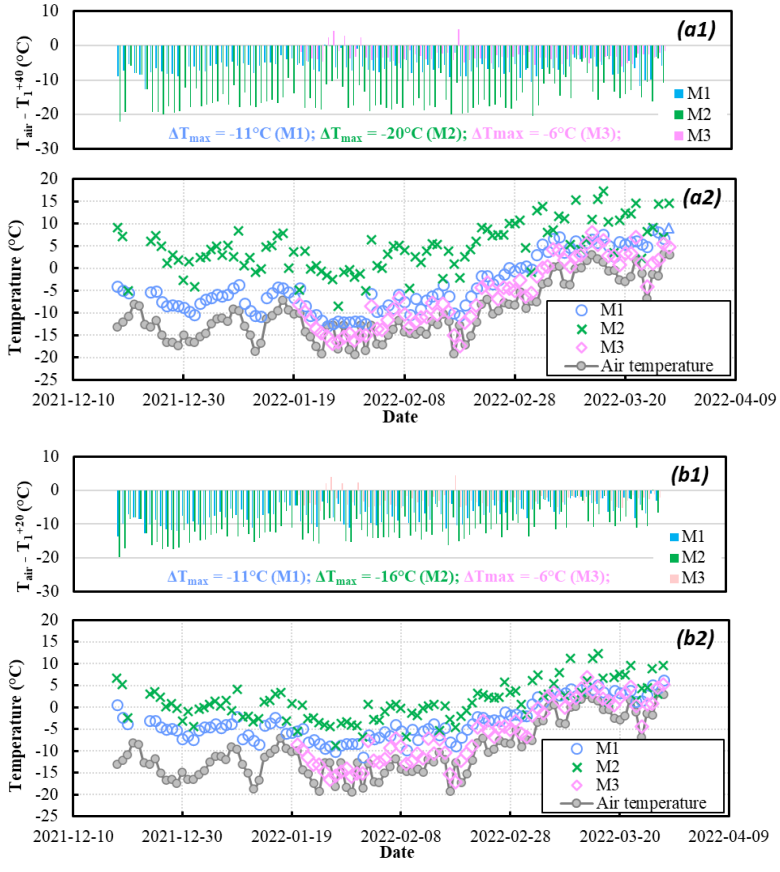

https://doi.org/10.5194/tc-2022-241
Preprint. Discussion started: 13 February 2023


The Cryosphere Discussions
Open Access
EGU

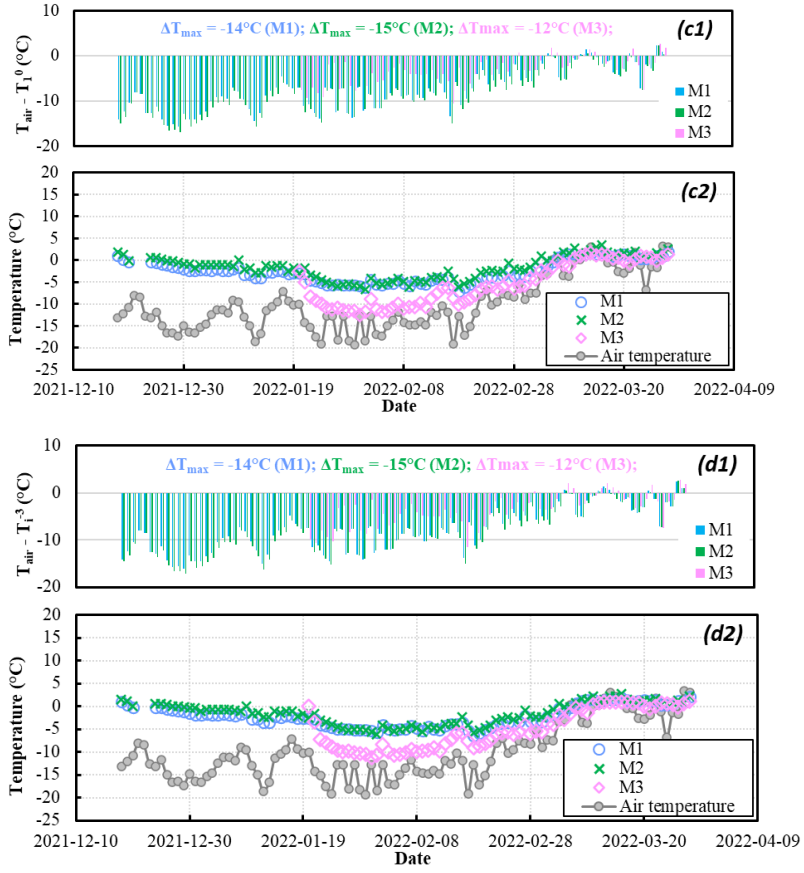


**Figure 3: Temporal and spatial variation of temperature at different elevations. (a2) and (b2) show the temperatures measured 40 cm ($T_{40}^i$) and 20 cm ($T_{20}^i$) above the water level, respectively, while (a1) and (b1) show the difference between air temperature and that measured at corresponding depths. (c2) and (d2) show the temperature measured at water surface ($T_0^i$) and 3 cm below the surface ($T_{-3}^i$), while (c1) and (d1) show the corresponding differences.**

It is also interesting to investigate the correlation between air temperature and temperatures close to ice surface, e.g., $T_{40}^i$, $T_{20}^i$, $T_0^i$, and $T_{-3}^i$. The temperatures at M3, $T^3$, have a relatively higher coefficient of determination ($R^2$) with air temperature, which was on average 0.89, while the average values of $R^2$ between $T_{air}$ and $T^3$, and $T_{air}$ and $T^3$ are approximately 0.73 and 0.53, respectively. As mentioned above, since monitoring stations M1 and M2 were very close to the deck, solar radiation has an obvious impact on the temperatures close to ice surface.

The temperatures above the ice surface at M1 had a relatively high coefficient than that at M2, as M1 was located at the north side of the deck, where solar radiation has a limited impact on the temperature sensors. Again, monitoring station M3 was away from the deck. The coefficient of determination was close to 0.91, showing $T^3$ is closely related to $T_{air}$.

The coefficient of determination was large for $T_{40}^i$ and $T_{20}^i$ when compared with that for $T_0^i$, and $T_{-3}^i$, resulting from the presence of snow, which can refrain solar radiation from affecting temperature below the ice. Therefore, temperature sensors should be placed at a certain distance from the reservoir shore or structures.

https://doi.org/10.5194/tc-2022-241
Preprint. Discussion started: 13 February 2023


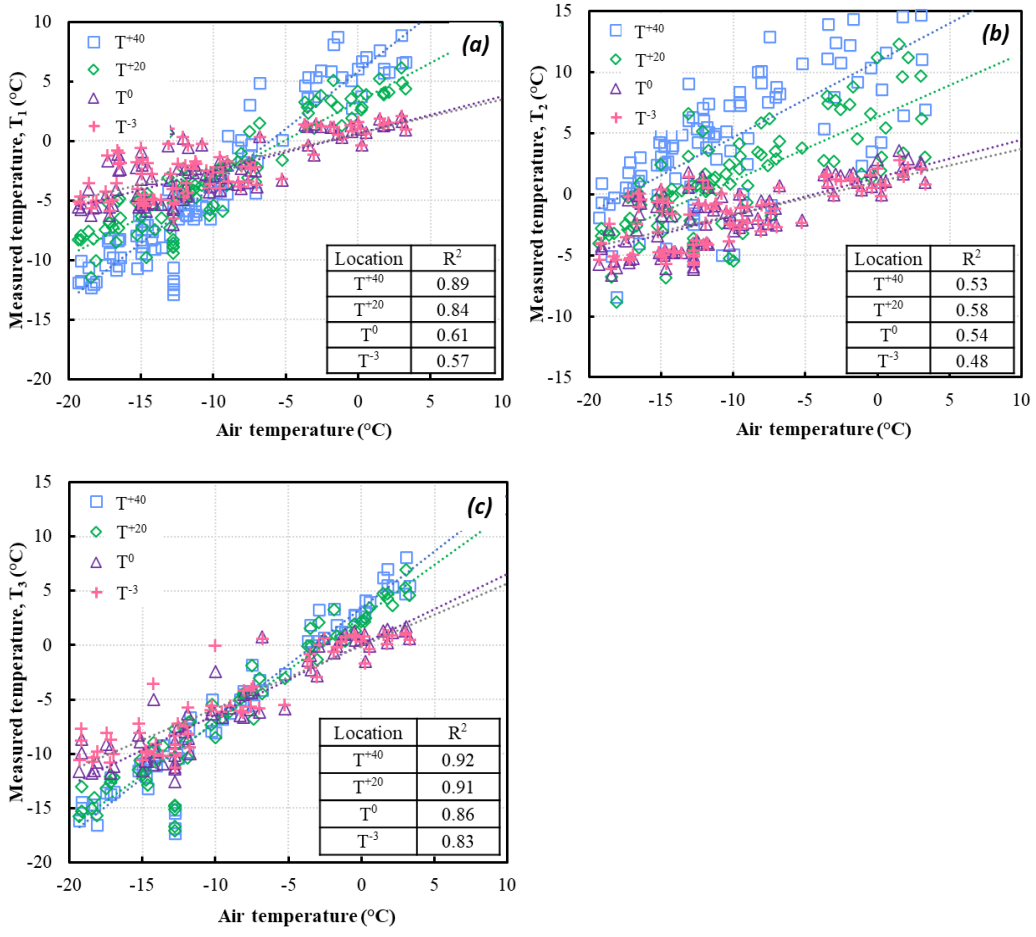


**Figure 4: Relationship between air temperature and temperatures close to ice surface at monitoring points (a) M1, (2) M2, and (3) M3.**

### 3.1.2 Temperature in ice

It is well known that ice temperature was below zero degrees. However, temperature gradient in the ice was rarely investigated. It is interesting to investigate the variation of the average temperature in the ice and the change of the temperature along the vertical profile in the ice.

Figure 5a show the variation of the temperature in 24 hours on January 01, 2022, February 01, 2022, and March 01, 2022. The average temperature was normalized by subtracting the average ice temperature at the beginning of every day. The temperature decreases to the lowest average temperature, which was observed approximately before sunrise, 10:00 am. The temperature then increased to the highest temperature detected before sunset, approximately, 18:00. Therefore, it can be concluded that the temperature of the ice was heavily affected by solar radiation, which agrees with the analysis in Section 3.1.

https://doi.org/10.5194/tc-2022-241
Preprint. Discussion started: 13 February 2023




To show the change of the temperature along the vertical profile, the temperature profile at the lowest temperature was shown in Figure 5b, which corresponds to the temperature at 10:00 am. The temperatures in the ice, together with ice thickness, were normalized to see the change of temperature along the vertical profile. The results showed that the lowest temperature was always detected at the ice surface and decreased along the ice depth. The increase rate of temperature was comparatively consistent. In addition, the regression line, with a correlation coefficient of 0.96 indicated temperature in ice increases with depth and can be estimated using a polynomial equation. Considering the impact of structure on solar radiation, the ice temperature at M3 indicated that normalized temperature was almost proportional to normalized ice thickness.

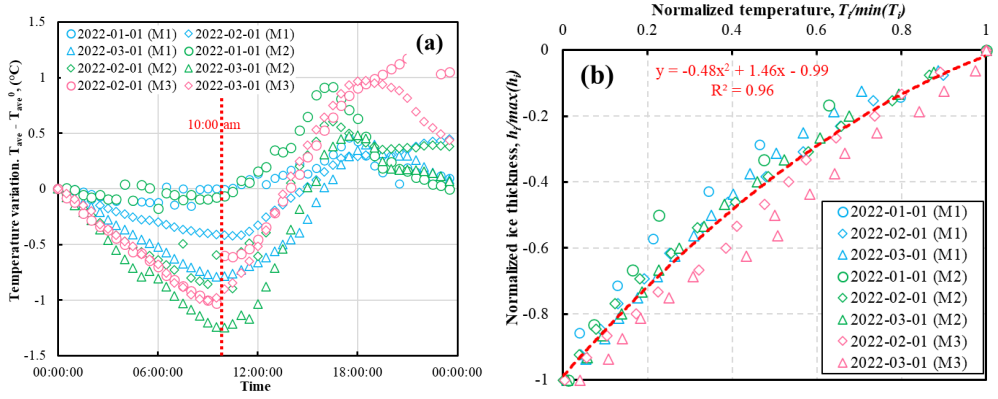


**Figure 5: Daily variation of temperature in the ice. (a) Variation of the average temperature of ice against time. (b) Variation of temperature along vertical profile in the ice shown in terms of normalized temperature against normalized ice thickness**

### 3.1.3 The amount of the temperature variation

Air temperature was mostly used to estimate the ice thickness. It is known that ice thickness varied within a day. Therefore, the correlation between the variation of the air temperature, $T_{air}$, and the temperatures close to the ice surface were investigated.

The maximum variation of air temperature was 26°C. The temperatures above the ice surface, $T_{40}$ and $T_{20}$, showed relatively large variations: approximately 39°C and 57°C at M1, 33 °C and 25°C at M2, 37 °C and 30 °C at M3, respectively. The variation of temperatures at M2 was always large than M1 and M3, resulting from the solar radiations. However, the variations of temperatures in all monitoring stations decreased from 40 cm to 20 cm above the ice surface. However, the variation of the temperatures close to the ice surface was proportional to $T_{air}$, although the rate was not the same at different elevations.

The variation of temperature below the ice surface was also proportional to $T_{air}$. However, the magnitude was comparatively small, which was less than 10°C. The difference in variations at M1 and M2 decreases at a deeper position. No significant difference was observed at all monitoring locations below ice surface, which was also appliable to average ice temperature.

https://doi.org/10.5194/tc-2022-241
Preprint. Discussion started: 13 February 2023


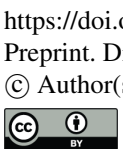

The Cryosphere Discussions
Open Access
EGU

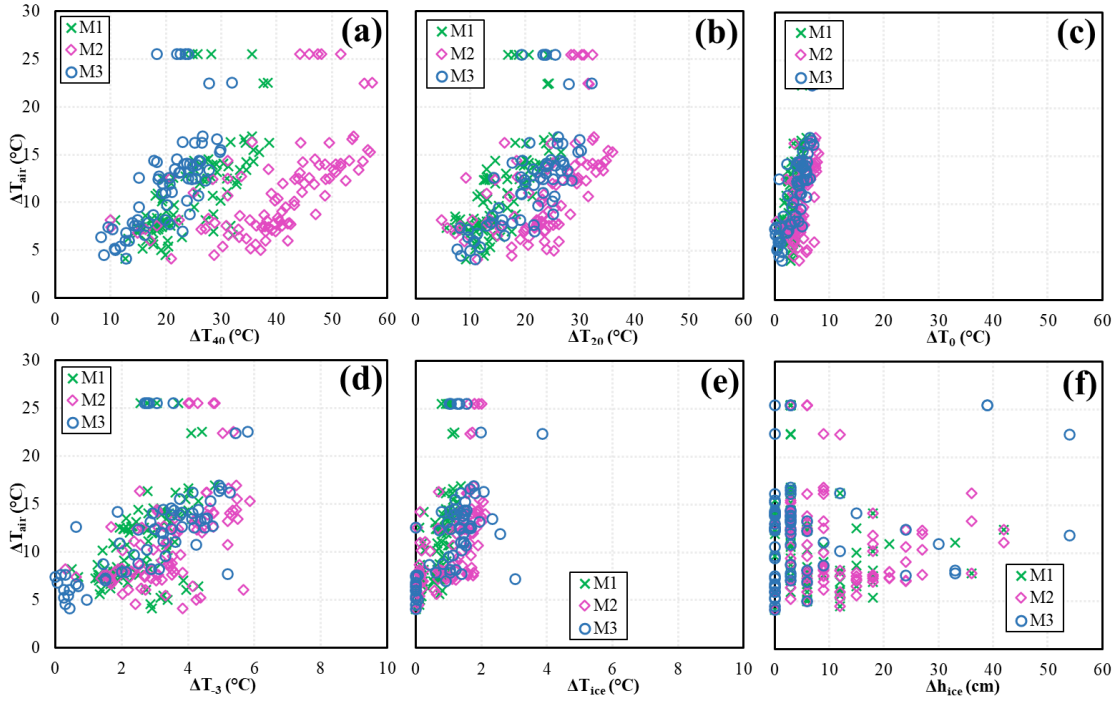


**Figure 6: Variation of temperatures close to ice surface and ice thickness against $\Delta T_{ai}$. (a) $\Delta T_{air}$ vs $\Delta T_{40}$; (b) $\Delta T_{air}$ vs $\Delta T_{20}$; (c) $\Delta T_{air}$ vs $\Delta T_0$; (d) $\Delta T_{air}$ vs $\Delta T_{-3}$; (e) $\Delta T_{air}$ vs $\Delta T_{ice}$; and (f) $\Delta T_{air}$ vs $\Delta h_{ic}$. Δ denotes the daily variation of temperature.**

### 3.2 Ice Thickness

Ice thickness was calculated based on the measured temperatures along the temperature arrays. As the spacing between temperature sensors below the ice surface was 3 cm, the resolution of the ice thickness was less than 3 cm. The accuracy of the measurement can be improved by decreasing the sensor spacing. However, the high intensity of the temperature sensor may interrupt the measurement results to a certain extent. Theoretically, ice thickness varies spatially and temporally. To simplify the calculation, averaged daily ice thickness was used in comparison with the variation in the day included.

#### 3.2.1 Calculated ice thickness vs time

The maximum daily ice thicknesses were 48, 50 and 55 cm at monitoring stations M1, M2 and M3, respectively, which were observed on February 22, 2022. Then the decaying process started until March 12, 2022. However, a refreezing process was noticed between March 13 and March 29, 2022, resulting from the decrease of air temperature in this period. Due to limited access, a hole was drilled on January 18, 2022, close to monitoring station M2, which revealed that ice thickness was approximately 28 cm at this station. The difference between the ice thickness observed and calculated was 1.75 cm. The first reason was the spacing between temperature sensors, which can be improved by decreasing the spacing. The second reason was that the average daily ice thickness was displayed in Figure 7. However, the ice thickness from the drilling hole was measured at a specific time.

https://doi.org/10.5194/tc-2022-241
Preprint. Discussion started: 13 February 2023




Stefan's model adopted AFDD to estimate ice thickness. Daily average ice thickness was used to calculate AFDD. The ice thickness in freezing and decaying processes were estimated. In the calculation, empirical coefficients, β and γ, were 0.017 and 0.5, respectively, according to Murfitt et al. (2018) and Comfort and Abdelnour (2013). The estimated maximum ice thickness was 60 cm observed on March 11, 2022, indicating discrepancies of 5 cm and 31 days in terms of thickness and time, respectively. Since daily temperature changes, daily maximum and minimum temperatures were also used to calculate the AFDD and ATDD, which were then used to estimate ice thickness. The calculated maximum ice thickness was 38 and 75 cm, while the discrepancies of starting the decaying process were 31 days in advance and 30 days late, based on the minimum and maximum daily temperatures, respectively.

Overall, the calculated ice thickness based on temperatures matches the ice thickness measured in the drilling hole. The estimated maximum ice thickness based on AFDD and ATDD was close to that measured according to ice temperature. The discrepancy between calculated and measured ice thickness was comparatively small, although the difference was observed on the date of maximum thickness.

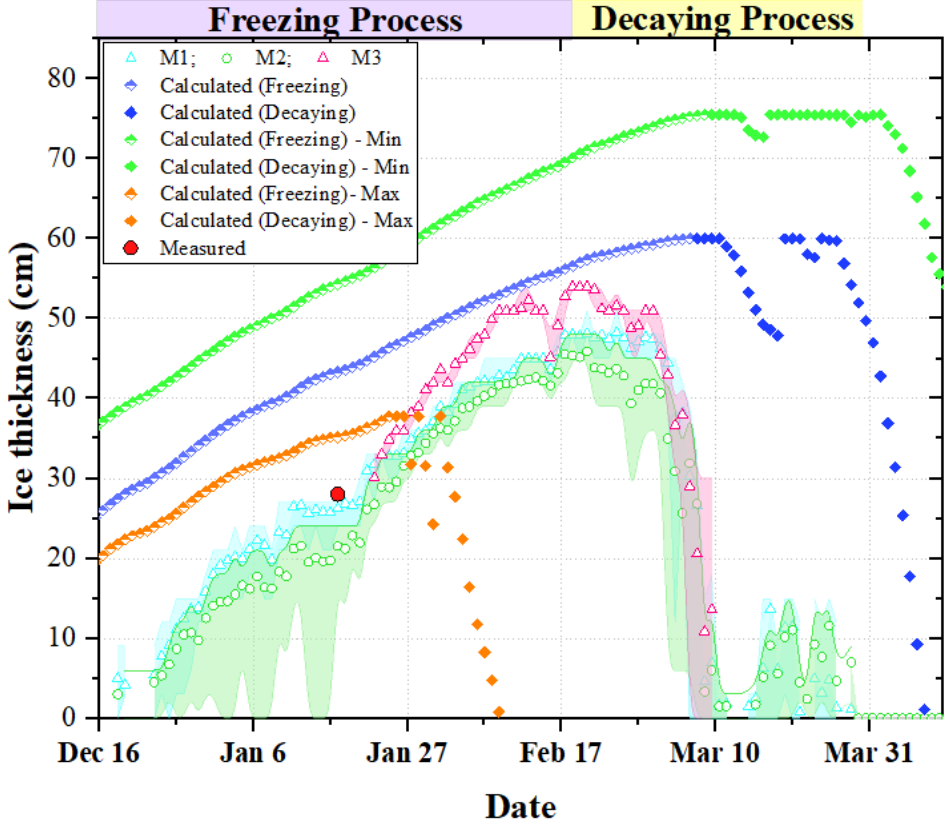


**Figure 7: Ice thickness measured based on the field observation and empirical models. As the spacings between temperature sensors are 3 cm, the calculated ice thickness should have a resolution of 3 cm as well.**

https://doi.org/10.5194/tc-2022-241
Preprint. Discussion started: 13 February 2023




### 3.2.2 Daily ice thickness variation

Figure 7 shows that the variation of the ice thickness varied with time. At the begging of the freezing process, the variation of ice thickness was up to 24 cm at the monitoring station M1. However, the variation of ice thickness dropped to approximately 6 cm before the decaying process. During this period, the average $T_{air}$ was between -12 and -20°C, which means the variation of $h_{ice}$ was refrained by the extreme low air temperature. Significant variation of ice thickness was detected at the end of the decaying process, indicating the variation of ice thickness was limited by air temperature, especially when air temperature varies around zero degrees.

The variation of ice thickness decreased from 22 cm to 5 cm from January to March 2022 (Figure 7), which occurred between approximately 12:00 pm and 20:00 pm in January and between 14:00 to 19:00 pm in March. A small variation in ice thickness and short duration for changing ice thickness were attributed to the duration of solar radiation.

The variation at M2 was comparatively large than that at M1 in January due to the location of the monitoring station, as mentioned before. However, when the ice becomes thicker, the variation in air temperature has a limited impact on the water below the ice. Therefore, the ice thickness varied in a small range. In addition, due to the short duration of daytime, the variation became smaller. Due to the spacing between temperature sensors, a deviation smaller than 3 cm cannot be detected, resulting in no change or variation in ice thickness.

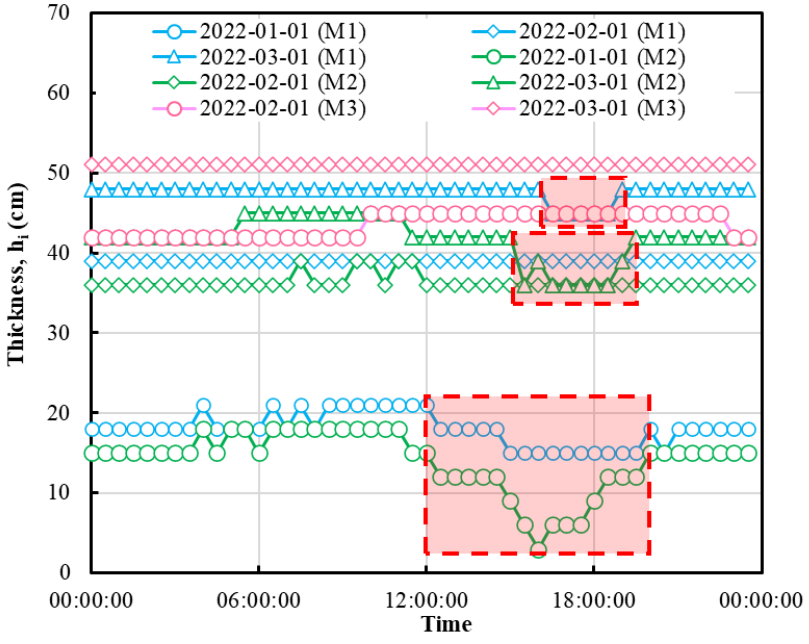


**Figure 8: Daily ice thickness at different locations**

The variation of ice thickness, approximately 57 cm in maximum, was impacted by air temperature, or it is also correct that the variation of ice thickness was attributed to the variation in air temperature (Figure 6f). However, the air temperature was not the only factor contributing to the ice formation. At least, ice thickness was not proportional to the air temperature at M1, M2 and M3. Therefore, other factors should be investigated as well.

https://doi.org/10.5194/tc-2022-241
Preprint. Discussion started: 13 February 2023




## 4 DISCUSSION

### 4.1 Pearson correlation analysis

Pearson coefficient of correlation is the measure of linear correlation between two sets of data, which is defined as the ratio between the covariance of two variables and the product of their standard deviations. However, it should be noted that the measure can only reflect a linear correlation of variables and ignores many other types of relationships or correlations.

In most of the empirical models, AFDD was introduced to estimate ice thickness. Although using AFDD can only obtain the average daily ice thickness, it still provides valuable information in understanding the freezing and decaying process. Instead of using one variable in estimating ice thickness, the correlation between ice thickness and other indices that can be easily measured was investigated. In this section, the parameters in correlation analysis consist of temperatures above the ice surface, $T_{air}$, $T_{40}$, $T_0$, and temperature below the ice surface, $T_{-3}$, $T_{ice(c)}$. Besides, the difference between $T_{air}$ and the above-mentioned temperatures, $T_{air}$-$T_{40}$, $T_{air}$-$T_0$, $T_{air}$-$T_{-3}$, were also included in the correlation analysis. Pearson correlation coefficients were calculated for the temperatures measured at M1, M2 and M3. In addition, all of the data were also included as a set of data for analysis (Figure 9).

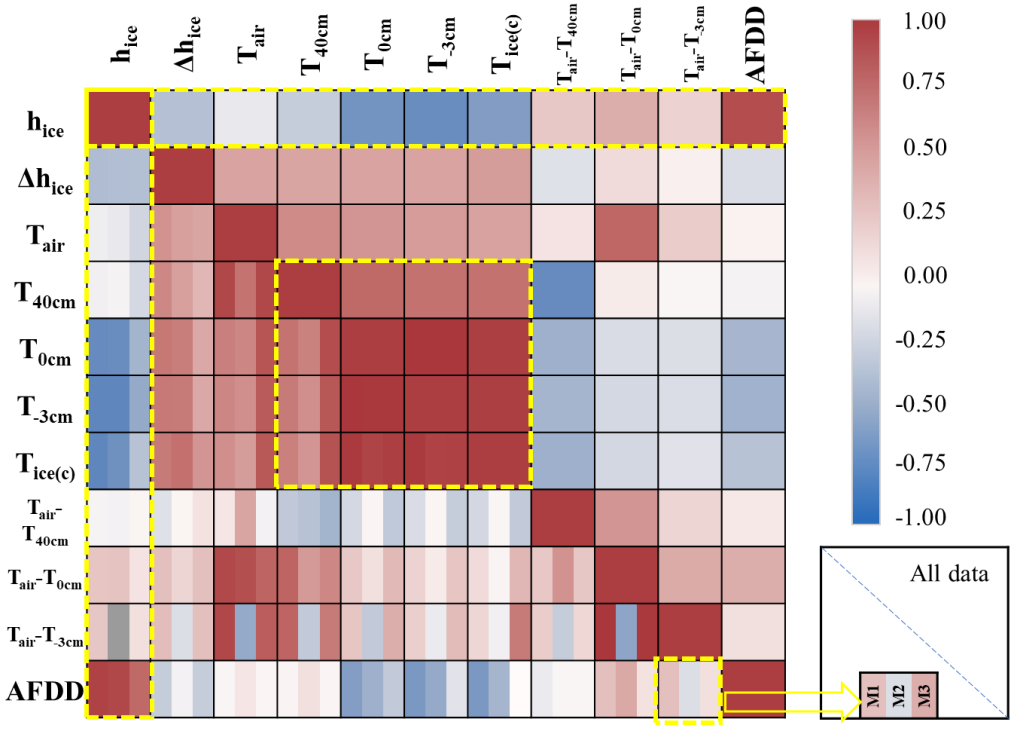


**Figure 9: Pearson Coefficient calculation of possible factors that contribute to freezing and decaying processes of ice**

There is a difference between the correlation coefficients at different monitoring stations, e.g., the correlation coefficient between $T_{air}$-$T_{-3}$ and $T_{air}$, which was 0.92 and 0.81 for the temperatures at M1 and M3 (Figure 9). However, a comparatively small correlation coefficient, -0.53, was obtained, resulting from the impact of solar radiation on the

https://doi.org/10.5194/tc-2022-241
Preprint. Discussion started: 13 February 2023




monitoring stations. The same phenomenon was observed for the correlation between $T_{air}$-$T_{-3}$ and $T_{air}$-$T_0$, $T_{air}$-$T_{-3}$ and $T_{40,}$ and $T_{air}$-$T_{-3}$ and $T_{air}$-$T_{40}$, demonstrating the correlation coefficient is sensitive to the data set. For the rest of the correlation coefficients, the overall range between two variables is very similar.

Although the correlation coefficient varies at different monitoring stations, the coefficients overall fall into the same range. Based on the correlation coefficients, it was noticed that the temperatures, $T_{40}$, $T_0$, $T_{-3}$, and $T_{ice(c)}$ are proportional to each other, especially for $T_0$, $T_{-3}$, and $T_{ice(c),}$ which has a correlation coefficient larger than 0.94 at all monitoring stations.

Figure 9 also indicates that ice thickness was proportional to AFDD with a coefficient of 0.89, and negatively correlated with $T_0$, $T_{-3}$, and $T_{ice(c)}$ with coefficients of -0.69, -0.73 and -0.62, respectively. The rest of the factors/indices are not closely related to ice thickness. However, since $T_{-3}$, and $T_{ice(c)}$ is measured or calculated based on the temperatures below the ice surface, $T_0$ was adopted in the following machine-learning process.

### 4.2 Regression analysis

As AFDD is a daily-based parameter, the temperatures used in machine learning were also daily-based. The monitoring information from all monitoring stations was included. Based on the correlation analysis, it is noticed that ice thickness is closely related to AFDD, and ice temperatures, $T_0$, $T_{-3}$, and $T_{ice(c)}$. However, considering the practical application, $T_0$ instead of $T_{40}$ was included in machine learning process.

In the machine learning process, three linear models and one non-linear model were introduced. In total, 241 group information was included in the machine learning process, with 80% of data points treated at training set and the rest of 20% treated as the test set. The indices used to evaluate the model performance include MAE, MSE and RMSE. Table 1 lists the variables in each model.

**Table 1: Summary of the models and best fit formulas in predicting ice thickness**

| Methods | Variables | Equations | No. |
|---|---|---|---|
| Linear-1 | $T_{air}$, $T_{40}$, $T_0$, AFDD | $h_{ice} = 0.151\times T_{air} +0.121\times T40-1.938\times T_0+0.031\times AFDD$ | (10) |
| Linear-2 | AFDD | $h_{ice} = 0.039\times AFDD$ | (11) |
| Linear-3 | $T_0$, AFDD | $h_{ice} =-1.569\times T_0+0.032\times AFDD$ | (12) |
| Non-Linear | β, $AFDD^{\gamma}$ | $h_{ice} = 0.06\times AFDD^{0.94}$ | (13) |

Figure 10a1 to Figure 10a4 display the correlation between ice thickness, $h_{ice}$ and other four parameters used in the machine learning process. It is clearly shown that $h_{ice}$ is comparatively well correlated with $T_0$ and AFDD. As the temperature at the ice surface in the freezing and decay processes was negative, the ice thickness was inversely proportional to $T_0$. Air temperature and temperature 40 cm above the ice surface was not well correlated with ice thickness.

https://doi.org/10.5194/tc-2022-241
Preprint. Discussion started: 13 February 2023


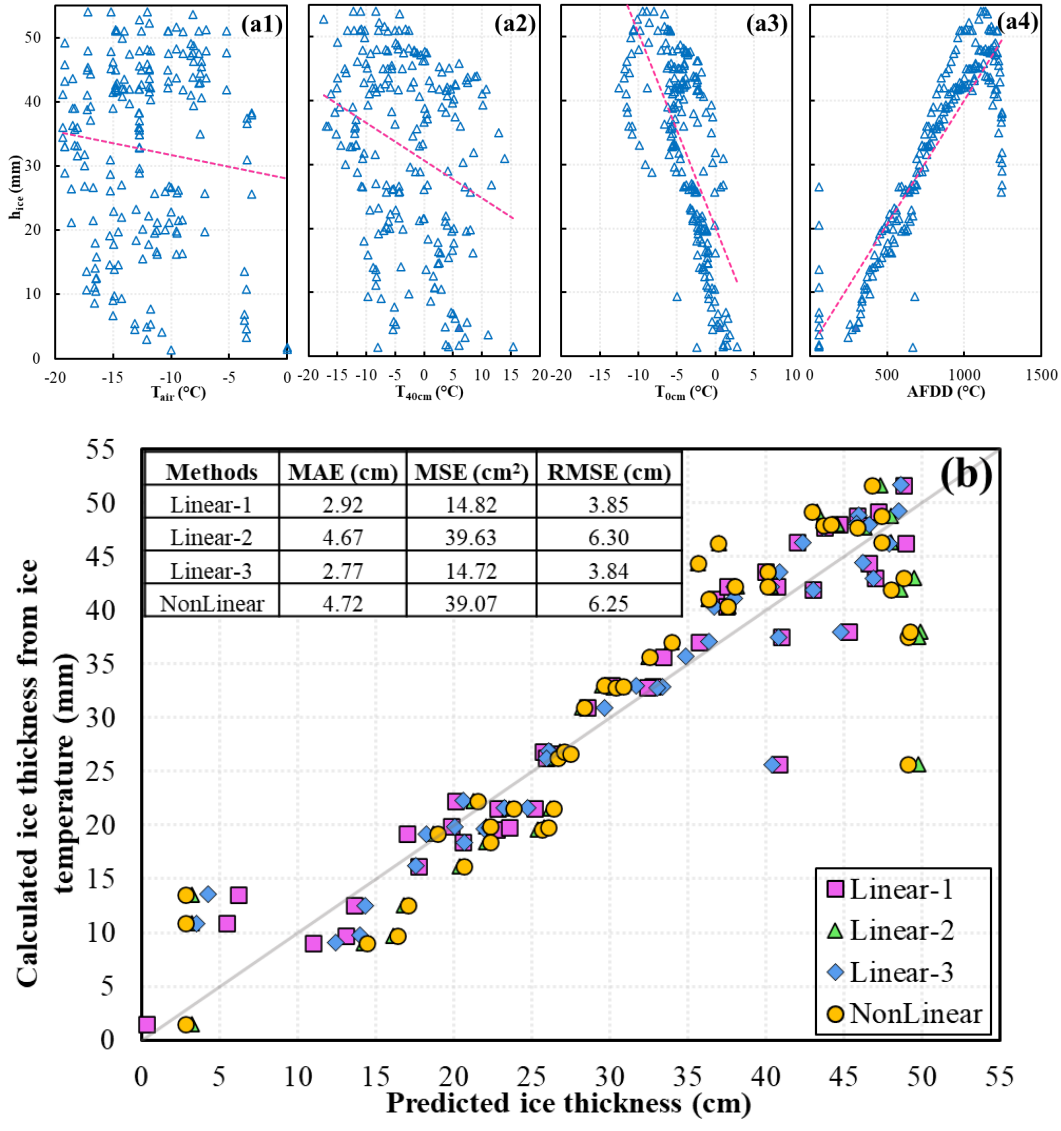


| Methods | MAE (cm) | MSE (cm²) | RMSE (cm) |
|---|---|---|---|
| Linear-1 | 2.92 | 14.82 | 3.85 |
| Linear-2 | 4.67 | 39.63 | 6.30 |
| Linear-3 | 2.77 | 14.72 | 3.84 |
| NonLinear | 4.72 | 39.07 | 6.25 |

**Figure 10: Summary of machine learning using nonlinear and linear modes. The discrepancies were also summarized in terms of MAE, MSE and RMSE. The corresponding functions were included in Table 2.**

Figure 10b showed that RMSE of ice thickness measured and calculated was ranging from 3.85 to 6.30 cm. The best-fit parameters in the training process were included in Table 2, and the corresponding discrepancies were included on Figure 10. It is obvious, the linear models with AFDD have a similar discrepancy as the nonlinear model with one variable, AFDD. The linear models with ice surface temperature incorporated (Linear-3) have a comparatively smaller discrepancy of 3.8 cm in terms of RMSE.

For the non-linear model, power law equation along with an empirical coefficient was trained and tested. The best-fit empirical coefficient was 0.06. Hicks (2016) mentioned that the empirical coefficient ranges from 0.017 to 0.024 for

https://doi.org/10.5194/tc-2022-241
Preprint. Discussion started: 13 February 2023


an average lake with snow cover. However, this empirical coefficient was based on $AFDD^{0.5}$, which means only one coefficient was used. In this study, the best fit magnitude of exponent was 0.96, larger than that used mostly.

Instead of using the artificial neural network method (Haq et al. 2021; Zaier et al. 2010), which required a hidden layer and more unknown parameters involved, a linear model with measurable parameters is a more practical approach for estimating ice thickness.

### 4.3 Validation of the proposed model

Temperature information from three monitoring stations was used to evaluate the performance of the proposed linear model 3 (LM-3) in Figure 10, which include Stations #1 (S1) and #2 (S2) located in Lake Baikal, Russia, and Station #3 (S3) located in Lake Kilpisjarvi, Finland (Aslamov et al. 2021). Since AFDD was needed in estimating ice thickness when Stefan's model was used, the air temperature information of S1 and S2 was from a meteorological station # 30710099999 (latitude 52.268028, longitude 104.388975) while air temperature of S3 was from meteorological station # 2701099999 (latitude 69.04541389, longitude 20.84879167). The available dataset of S1 and S2 are from February 02 to March 25 in 2017, and S3 is from January 21 to April 18. 2018. Ice thicknesses for S1, S2 and S3 range from 23.2 to 46.0 cm, 24.8 to 58.9 cm and 50.5 to 76.6 cm, respectively.

Ice thickness was calculated based on the simplified Stefan's model, which is proportional to the square root of AFDD with an empirical coefficient included ranging from 0.017 to 0.024 for an average lake with snow cover (Hicks 2016). In the calculation, the calculation results associated with the coefficient of 0.024 refer to the upper boundary (UB), and 0.017 refer to the lower boundary (LB). The discrepancies between the calculated ice thickness and measured ice thickness were shown in terms of RMSE since MAE, MSE, and RMSE showed consistent results in Figure 10. Figure 11 shows the results of calculated ice thickness at stations S1, S2 and S3. The calculated ice thicknesses in monitoring stations M1, M2 and M3 were included for comparison. The results showed that RMSE between the results from the linear model and measured ice thickness for both S1 and S2 is smaller than that from Stefan's models for both UB and LB. Similar conclusion was made at stations in this study.

However, for the ice thickness data from Lake Kilpisjarvi (S3), the RMSE between model LM-2 was between the RMSEs of UB and LB. The magnitude of RMSE of LB showed that the ice thickness calculated using LB was close to the measured ice thickness. However, this observation was not consistent for S1, S2, and all stations in this paper. The main reasons are the difference between the measured air temperature 1.5 m above the ice surface at the monitoring station and temperatures from meteorological stations, which resulted in the discrepancies of AFDD. Air temperature in this study overall was close to the monitoring stations. Therefore, RMSE was comparatively small, which was only 3.8 cm.

In Stefan's model, it was considered that $T_{air}$ was equal to $T_{air}$, which is not accurate based on this study. It means that heat flux was omitted (Zhaka et al. 2021). In addition, based on the calculated ice thickness and comparison results, it is concluded that the limitations of the Stefan's model are the model didn't consider the variation of ice thickness spatially and temporally. A meteorological station was generally away for monitoring stations. Therefore, the variation of air temperature spatially as a result of the change of elevation and solar radiation was not considered. Also, the local environment may have an impact on the air temperature. Therefore, a model with local air temperature or ice

https://doi.org/10.5194/tc-2022-241
Preprint. Discussion started: 13 February 2023




surface temperature included should be used, which is one of the advantages of the linear model. Another advantage of the linear model was that instead of using two unknown coefficients with a range in Stefan's model, two constants were given in LM-3 to estimate ice thickness. From analyzing the results of stations S1, S2, and S3 and all stations in this paper, the discrepancy was very consistent. The linear model, LM-3, can even be improved if sufficient air temperature and ice temperatures are available for an area by following the research approach in this paper. However, a significant difference was not expected.

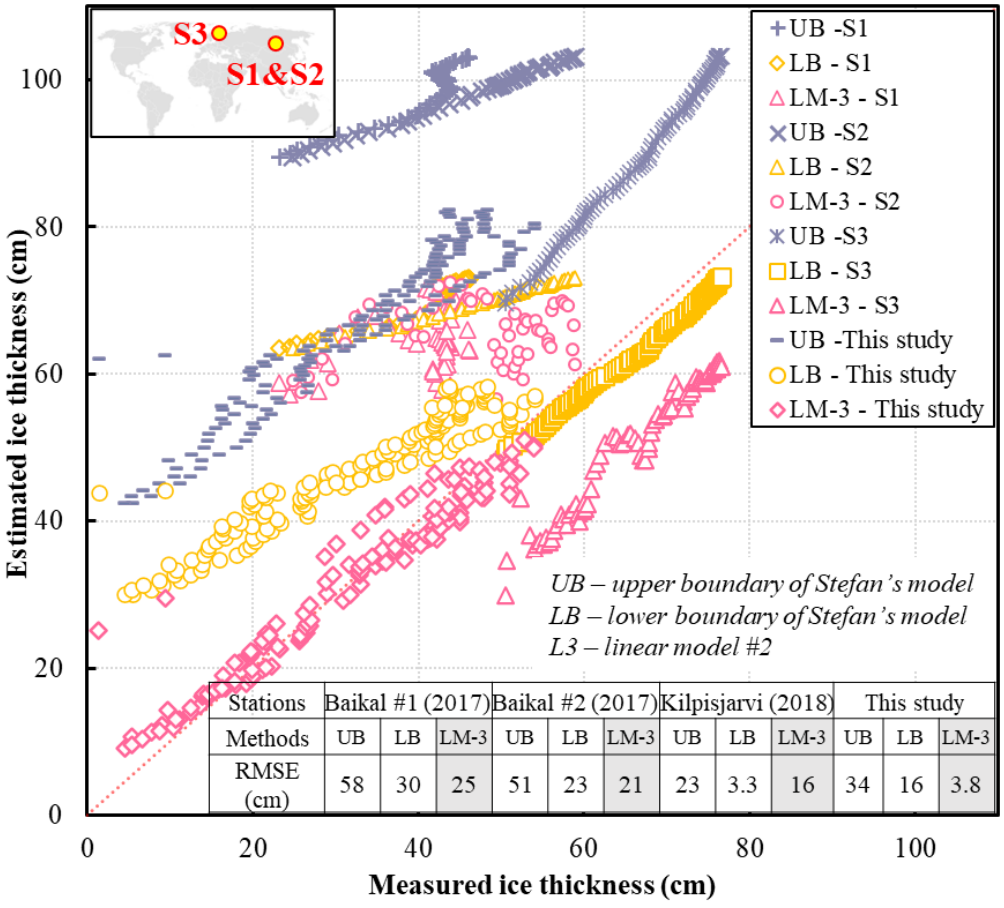


| Stations | Baikal #1 (2017) | | | Baikal #2 (2017) | | | Kilpisjarvi (2018) | | | This study | | |
|---|---|---|---|---|---|---|---|---|---|---|---|---|
| Methods | UB | LB | LM-3 | UB | LB | LM-3 | UB | LB | LM-3 | UB | LB | LM-3 |
| RMSE (cm) | 58 | 30 | 25 | 51 | 23 | 21 | 23 | 3.3 | 16 | 34 | 16 | 3.8 |

**Figure 11: Evaluation of the proposed linear model and comparison with Stefan's model. In the comparison, the recommended range of the empirical coefficient was incorporated through upper and lower boundaries. In addition, the comparison results were presented in terms of RMSE the ice thickness.**

## 5 CONCLUSION

In this paper, temperature information collected at three monitoring stations (M1, M2 and M3) was used to study the ice freezing and thawing processes on a reservoir along Irtysh River. Temperatures above and below ice surface were

https://doi.org/10.5194/tc-2022-241
Preprint. Discussion started: 13 February 2023


comprehensively analyzed and correlated with air temperature. Ice thicknesses were calculated based on measured temperatures along monitoring arrays at M1, M2 and M3 and compared with that calculated using simplified Stefan's model. The calculated ice thickness was further correlated with temperatures, variations of temperature and accumulated freezing degree days (AFDD) based on Pearson correlation analysis and linear and non-linear models were proposed, which were validated using dataset from three stations (S1, S2 and S3) in Russian and Finland.

Through analyzing air temperature and measuring temperatures close to the ice surface and in the ice, it was noticed that the temperature close to the ice surface was closely related to $T_{air}$ for M3, not M1 and M2. The lowest temperature was noticed before sunrise and the highest temperature was before sunset. In addition, the temperature in ice almost increases linearly with depth.

The maximum daily ice thicknesses were 48, 50 and 55 cm at monitoring stations M1, M2 and M3, respectively, which were observed on February 22, 2022. The measured ice thickness from the drilled hole was close that calculated based on ice temperature. The maximum calculated ice thickness using Stefan's model was 60 cm observed on March 11, 2022, indicating discrepancies of 5 cm and 31 days in terms of thickness and time, respectively. The variation of ice thickness occurred in the afternoon and when the ice became thicker, ice thickness varied in a comparatively small range.

Pearson coefficient of correlation was adopted to study the potential correlations between ice thickness and air temperatures. Temperatures $T_{40}$, $T_0$, $T_{-3}$, and $T_{ice(c)}$ are proportional to each other, especially for $T_0$, $T_{-3}$, and $T_{ice(c)}$ which have a correlation coefficient larger than 0.94 at all monitoring stations. Ice thickness was proportional to AFDD with a coefficient of 0.89, and negatively correlated with $T_0$, $T_{-3}$, and $T_{ice(c)}$ with coefficients of -0.69, -0.73 and -0.62, respectively. The results of regression analysis showed that linear model #3 (LM-3) with ice surface temperature incorporated has a comparatively smaller discrepancy between measured and calculated ice thickness.

LM-3 was also validated using the dataset from S1, S2 and S3, showing that the proposed model L2 has the capacity to capture the local ice freezing and thawing processes with a relatively small discrepancy, and the results were consistent between different stations. The paper provides an approach to study the ice freezing and thawing processes comprehensively and a practical model to calculate ice thickness with air temperature and temperature at the ice surface incorporated.

https://doi.org/10.5194/tc-2022-241
Preprint. Discussion started: 13 February 2023




## AUTHOR CONTRIBUTION

Chuntan Han, Chengxian Zhao and Jianhua Luo were in charge of data curation. Chuntan Han and Chao Kang designed the methodology of monitoring and analysis. Chao Kang developed the model code and performed the simulations. Rensheng Chen supervised the monitoring process and paper preparation.

https://doi.org/10.5194/tc-2022-241
Preprint. Discussion started: 13 February 2023




460 **ACKNOWLEDGEMENTS**

This research was supported by the National Key R&D Program of China (grant number 2019YFC1510502), technical Service Project of Irtysh River of Xinjiang Investment and Development (Group) Co. LTD (grant numbers KKYG08/2021), the National Natural Science Foundation of China (grant numbers 41971041).

https://doi.org/10.5194/tc-2022-241
Preprint. Discussion started: 13 February 2023




465 **DATA AVAILABILITY STATEMENT**

All data, models, and code generated or used during the study appear in the submitted article.

https://doi.org/10.5194/tc-2022-241
Preprint. Discussion started: 13 February 2023




## COMPETING INTERESTS

The authors declare that they have no conflict of interest.

470

https://doi.org/10.5194/tc-2022-241
Preprint. Discussion started: 13 February 2023




**REFERENCE**

Akyurt, M., Zaki, G. and Habeebullah, B., 2002. Freezing phenomena in ice–water systems. Energy conversion and management, 43(14), 1773-1789.

Alexiades, V. and Solomon, A.D., 2018. Mathematical modeling of melting and freezing processes. Routledge.

Aslamov, I., Kirillin, G., Makarov, M., Kucher, K., Gnatovsky, R. and Granin, N., 2021. Autonomous System for Lake Ice Monitoring. Sensors, 21(24), 8505.

Bilello, M.A., 1960. Formation, growth, and decay of sea ice in the Canadian Arctic Archipelago (Vol. 65). US Army Snow Ice and Permafrost Research Establishment, Corps of Engineers.

Bouaanani, N., Paultre, P. and Proulx, J., 2004. Dynamic response of a concrete dam impounding an ice-covered reservoir: Part I. Mathematical modelling. Canadian Journal of Civil Engineering, 31(6), 956-964.

Braga, S.L. and Milón, J.J., 2012. Visualization of dendritic ice growth in supercooled water inside cylindrical capsules. International Journal of Heat and Mass Transfer, 55(13-14), 3694-3703.

Cao XW. (2021), Observation and simulation research on growth and decay processes of ice cover on lake Wuliangshuihai. PhD thesis, Dalian: Dalian University of Technology.

Cao, X., Li, Z., Wang, Q., Wang, J. and Li, G., 2017. Estimation of Lake Ice Thickness Using Measured Temperature Profile in Ice and Water. In Proceedings of the International Conference on Port and Ocean Engineering Under Arctic Conditions.

Comfort, G. and Abdelnour, R., 2013, July. Ice thickness prediction: a comparison of various practical approaches. In Proceedings 17th CRIPE Workshop on River Ice (329-342).

Deng, X., Cheng, Y., Li, L., Feng, J., Cui, L., Du, C., Zhang, L., Zhang, L. and Qin, J., 2020. Design and application of high-precision temperature measuring instrument for ice cover profile of river based on the resistance residual compensation method. IEEE Access, 8, 7899-7906.

Ding, F.L., and Mao Z.Y. (2021), Study on thermal ice stresses of a pond in cold region, *Engineering Mechanics*, 38 (9), 239-245, 56.

Hao YS., Deng X., Gui LQ., Qin JM., Zhang L., Shen XQ., Shi Y. (2017), Research on the waterways ice thickness discrimination algorithm based on the characteristics of ice temperature gradient. Yellow River, 39 (10), 32-35.

Haq, M.A., Azam, M.F. and Vincent, C., 2021. Efficiency of artificial neural networks for glacier ice-thickness estimation: A case study in western Himalaya, India. Journal of Glaciology, 67(264), 671-684.

Hellgren, R., Malm, R., Fransson, L., Johansson, F., Nordström, E. and Wilde, M.W., 2020. Measurement of ice pressure on a concrete dam with a prototype ice load panel. Cold Regions Science and Technology, 170, p.102923.

Hicks, F. 2016. An Introduction to River Ice Engineering: for Civil Engineers and Geoscientists. Committee on River Ice Processes and the Environment, Canadian Geophysical Union, Hydrology Section, Edmonton, AB.

Howell, S.E., Laliberté, F., Kwok, R., Derksen, C. and King, J., 2016. Landfast ice thickness in the Canadian Arctic Archipelago from observations and models. The Cryosphere, 10(4), 1463-1475.

https://doi.org/10.5194/tc-2022-241
Preprint. Discussion started: 13 February 2023




Kobler, U.G. and Schmid, M., 2019. Ensemble modelling of ice cover for a reservoir affected by pumped-storage operation and climate change. Hydrological Processes, 33(20), 2676-2690.

Lebedev, V.V., 1938. Rost l'da v arkticheskikh rekakh i moriakh v zavisimosti ot otritsatel'nykh temperatur vozdukha. Problemy arktiki, 5(6), 9-25.

Murfitt, J.C., Brown, L.C. and Howell, S.E., 2018. Estimating lake ice thickness in Central Ontario. PLoS One, 13(12), e0208519

Otto, J.C., Helfricht, K., Prasicek, G., Binder, D. and Keuschnig, M., 2022. Testing the performance of ice thickness models to estimate the formation of potential future glacial lakes in Austria. Earth Surface Processes and Landforms, 47(3), 723-741.

Stefan, J., 1890. Uber die Theorie der Eisbildung in Spesondere u ber Eisbilding im Polarmeer Stiz. Ber. Kais. Akad. Wiss. Wein, 98(2A), p.965.

Werder, M.A., Huss, M., Paul, F., Dehecq, A. and Farinotti, D., 2020. A Bayesian ice thickness estimation model for large-scale applications. Journal of Glaciology, 66(255), 137-152.

Xie, F., Lu, P., Li, Z., Wang, Q., Zhang, H. and Zhang, Y., 2022. A floating remote observation system (FROS) for full seasonal lake ice evolution studies. Cold Regions Science and Technology, 199, 103557.

Zaier, I., Shu, C., Ouarda, T.B., Seidou, O. and Chebana, F., 2010. Estimation of ice thickness on lakes using artificial neural network ensembles. Journal of Hydrology, 383(3-4), 330-340.

Zhaka, V., Bridges, R., Riska, K. and Cwirzen, A., 2021. A review of level ice and brash ice growth models. Journal of Glaciology,1-20.